Nonchaotic behavior in the Josephson junction

Mark Levi

Department of Mathematics, Boston University, Boston, Massachusetts 02215

(Received 26 February 1987; revised manuscript received 29 July 1987)

Using geometric arguments of nonlinear dynamics we determine parameter regions for which the resistively shunted Josephson equation is assuredly nonchaotic, with or without an inductive shunting term, and with *any forcing*. These results can account for the observed stability and voltage-to-frequency fidelity of the Kamper-Soulen resistively shunted Josephson thermometer, in the region of low inductive shunting.

I. INTRODUCTION

The aim of this note is to illustrate on a specific example a general method for proving the "lack of chaos" in various forced oscillators. We concentrate on the example of the Josephson's equation describing the phase jump ϕ across a resistively shunted Josephson junction, with or without inductive shunting. This equation in dimensionless form is given by

$$\beta\ddot{\phi}+(1+\gamma\cos\phi)\dot{\phi}+\sin\phi=p(t) , \qquad (1)$$

where β and γ are parameters and $p(t)$ is periodic of period $T=2\pi/\omega$. The case of linear damping: $\gamma=0$ corresponds to the damped pendulum with torque,

$$\beta\ddot{\phi}+\dot{\phi}+\sin\phi=p(t) . \qquad (2)$$

There is no loss of generality in assuming special coefficients for $\dot{\phi}$ and $\sin\phi$; the form (2) can be achieved by rescaling the dependent function and by rescaling and translating the time. This equation provides also a phenomenological model for some features of the charge-density waves.[1,2] We will prove in particular that Eq. (2) possesses a globally attracting invariant circle, provided only that $\beta<\frac{1}{4}$, with no other assumptions. The exact statement for Eq. (1) is given in theorem 1 below. The method used here applies to other systems as well.

Relation to previous studies

A number of authors[3-11] have used circle maps to describe the dynamics of (1) and (2). These studies are based on numerical and experimental evidence suggesting that the dynamics are one dimensional. We provide a rigorous foundation for this for a specific range of parameters.

The result of theorem 1 provides also the first rigorous step in the direction of establishing the bounds (in parameter space) on the chaotic behavior of the Josephson equation (see the recent work by Kautz and Monako[8]).

To connect our theoretical result with some previous numerical studies, we rescale Eq. (2) by changing time $t=\sqrt{\beta}\tau$, obtaining

$$\phi''+G\phi'+\sin\phi=q(t) , \quad '=\frac{d}{dt} , \quad q(\tau)=p(\sqrt{\beta}t) ,$$

where $G=\beta^{1/2}$.

Our condition $\beta<\frac{1}{4}$ is equivalent to $G>2$. Chaos has been found in Eq. (2) for G as high as 1.576,[3] which shows that $G>2$ is not too crude an estimate. According to the simulation study in Ref. 9, Eq. (2) reduces to an invertible one-dimensional (1D) circle map for $\beta=0.029$, assuming a certain form of forcing. Theorem 1 below actually predicts this result rigorously for *any* $\beta<0.25$ and for *any* forcing. The estimate $\beta\ll1$ which was proposed on the empirical basis[8,12] is made precise here. We also establish the validity of the last connection in the diagram drawn in Ref. 5:

physical system$\rightarrow$ Eq. (2)$\rightarrow$2D Poincaré map

$$\rightarrow \text{1D invertible circle map} .$$

In an experimental study[13] Tao et al. deduce the existence of chaotic behavior in a resistively shunted junction circuit for $\beta\ll1$. This result contradicts theorem 1 if $\beta<1/4$. A possible resolution of this contradiction can be the presence of some extraneous effects (e.g., inductive shunting, or external noise) not accounted for in the authors' model. Finally, note that our result explains the stability and voltage-to-frequency fidelity of the resistivity shunted Josephson noise thermometer in the region of low inductive shunting.

II. RESULTS AND DISCUSSION

The first reduction-of-dimension result in the context of periodically forced oscillations is due to Levinson.[14] It is a perturbation theorem stating in effect that for small periodic forcing of a planar autonomous system with a stable limit cycle the Poincaré map possesses an attracting invariant circle. In other words, an exponentially stable invariant circle of a map persists under sufficiently small perturbations of the map.

Levinson's theorem is not specific as to the allowed size of perturbations, but rather requires that these be sufficiently small. Theorem 1 below requires more but also gives more; in particular, the allowed size of perturbations is specified. Levinson's theorem can be applied to any forced oscillator with *weak* forcing, provided that the unperturbed version has a stable limit cycle.[15,16] Our theorem is different in that it allows one to *specify* a range of parameters for which the invariant circle still persists.

To state the main result of this note we write Eq. (1) as a system

$$\dot\phi = \frac{1}{\beta}[\psi - \Phi(\phi)] \ , \quad \Phi = \phi + \gamma \sin\phi \ ,$$

$$\dot\psi = -\sin\phi + p(t) \ , \quad p(t+T) = p(t) \ , \quad T = 2\pi/\omega \tag{3}$$

and define the Poincaré ("stroboscopic") map P as the period map taking $x = (\phi,\psi)_{t=0}$ into $Px = (\phi,\psi)_{t=2\pi/\omega}$. We shall treat the phase space $\{x\} = \{(\phi,\psi)\}$ as the cylinder by identifying each point (ϕ,ψ) with its 2π translates $(\phi + 2\pi n, \ \psi + 2\pi n)$. Equation (3) is clearly invariant under such translations. Thus Poincaré map P of the plane satisfies $P(\phi + 2\pi, \ \psi + 2\pi) = P(\phi,\psi) + (2\pi, 2\pi)$ and therefore gives rise to the map $\hat P$ of the cylinder.

Theorem 1. For any choice of non-negative parameters β and γ satisfying

$$0 \le \gamma < 1 \ , \quad 0 < \beta < 1/4(1-\gamma)^2 \ , \tag{4}$$

the Poincaré map $\hat P$ of the phase cylinder of Eq. (3) possesses a globally attracting invariant circle C given by $\psi = f(\phi) = f(\phi;\beta,\gamma,p)$, with $f(\phi + 2\pi) = f(\phi) + 2\pi$ (Fig. 1). Furthermore, $f(\phi)$ satisfies

$$\beta\frac{m-1}{1+\gamma} < f(\phi) - \Phi(\phi) < \beta\frac{M+1}{1-\gamma} \ ,$$

where $m = \min p(t)$, $M = \max p(t)$, $\Phi(\phi) = \phi + \gamma \sin\phi$. The function $f(\phi)$ is k times differentiable with $k \ge c/\beta$, where $c = c(\gamma)$ is a constant independent of β and $p(t)$. In particular, smaller β results in smoother invariant circles.

Remark 1. For the particular case of the simple driven damped pendulum, $\gamma = 0$, the above condition becomes simply $\beta < \frac{1}{4}$.
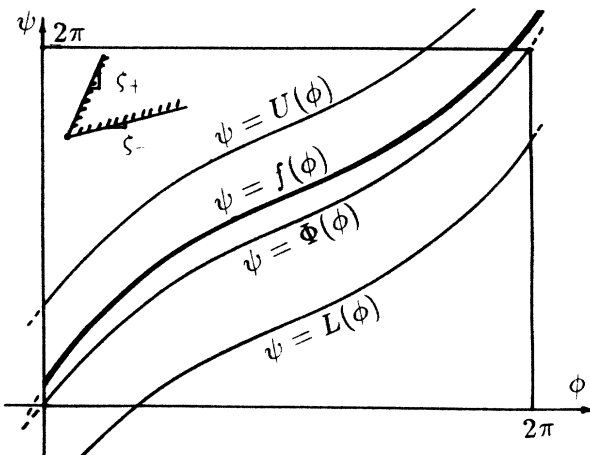
A. Dynamical consequences of the existence of the invariant circle

The existence of an attracting smooth invariant circle for the map $\hat P$ implies that the observed behavior of the system will be either periodic (if the rotation number $r = p/q$ is rational) or quasiperiodic (if r is irrational),[14,15] and thus certainly nonchaotic.

The significance of the rotation number lies in the fact that it carries most of the information on the qualitative behavior of the circle map and thus on the physical system. If $r = p/q$ is rational, then every solution will be or will tend to a $p:q$ phase-locked periodic subharmonic. In practice, every transient will quickly settle into a periodic mode. For the *irrational* rotation number all solutions starting on the invariant circle are quasiperiodic with two incommensurate basic frequencies ω and $r\omega$. Each such solution is of the form $\phi(t) = f(r\omega t, \omega t)$, where $f(x,y)$ is a function 2π periodic in both arguments.

Remark 2. The existence of the rotation number for invertible circle maps and its independence of the initial point has an important physical consequence. It is not hard to check that $r = \langle \dot\phi \rangle/\omega$, where $\langle \ , \ \rangle$ denotes the time average (which therefore exists); consequently, if there is a globally attracting invariant circle, then the voltage $r\omega$ is independent of the initial state of the system, a condition desirable in a measuring device.

B. Parametric dependence; Arnold tongues

Parametric dependence of the rotation number, and hence of the voltage (e.g., on i_0 if $p = i_0 + i_1\sin\omega t$), is described by the "devil's staircase," with plateaus corresponding to the lock-in modes. To understand the invertible circle maps completely, one has to look at the dependence on *two parameters*, one controlling the nonlinearity, the other controlling the tendency to rotate, such as ϵ and ω in the standard example $\alpha \to \alpha + \omega + \epsilon \sin\alpha$. If we have $p(t) = i_0 + i_1\sin\omega t$ in Eq. (2), then i_0 and i_1 serve as a natural choice of parameters. The bifurcation diagram with Arnold tongues is shown in Fig. 2. Several dynamical consequences can be seen from that diagram.

First, if we fix a *small* amplitude i_1, then the relative measure of the set of values of i_0 for which ω is irrational is close to 1. The same conclusion is true if we fix a large drift i_0. This implies that most solutions observed will be quasiperiodic if the drift is large or the amplitude is small.

Second, fixing amplitude i_1 and plotting r versus i_0 results in the devil's staircase with very short plateaus, resembling a smooth curve, Fig. 2(b). For i_0 large the

FIG. 1. $\psi = f(\phi)$ gives the invariant circle; $\psi = U(\phi)$, $\psi = L(\phi)$ give the boundaries of the strip S; $\Phi(\phi) = \phi + \gamma \sin\phi$.
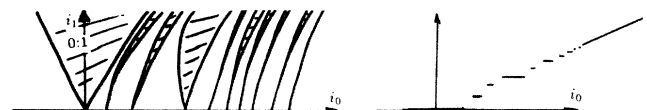
FIG. 2. "Arnold tongues" and the devil's staircase.

curve approaches a straight line implying a *near-Ohmic* *I-V* characteristic. A detailed explanation and proof of this fact will appear elsewhere. Proof of theorem 1 relies on the following simple and general fact.

Theorem 2. If a C^1 map $P: \mathbb{R}^2 \to \mathbb{R}^2$ subject to periodicity conditions $P(\phi + 2\pi, \psi + 2\pi) = P(\phi, \psi) + (2\pi, 2\pi)$ satisfies conditions (i) and (ii) below, then it possesses an invariant curve given by $\psi = f(\phi)$ with $f(\phi + 2\pi) = f(\phi) + 2\pi$; the corresponding cylinder mapping $\hat{P}$ has therefore an invariant circle. This curve is globally attracting in $\mathbb{R}^2$ and is unique.

Conditions. Two conditions for theorem 2 follow (see Fig. 1).

(i) P possesses an invariant bundle of horizontal sectors; that is, there exists two constants $\zeta_+ > \zeta_-$ such that any tangent vector (ξ_0, η_0) over any $x \in \mathbb{R}^2$ with the slope $\zeta_- < \eta_0/\xi_0 < \zeta_+$ maps under dP_x into the tangent vector (ξ_1, η_1) with $\zeta_- < \eta_1/\xi_1 < \zeta_+$. Here dP_x denotes the derivative matrix of the map P calculated at the point x.

(ii) P contracts area: there exists a constant $c > 0$ such that $|\det dP_x| \le c < 1$ for all $x \in \mathbb{R}^2$.

C. Heuristic discussion of the sector condition (i)

In physical terms, it is the *inertial effects* that allow for the possible chaotic behavior. High damping moderates such effects; our result makes this vague idea precise. Small β means large damping, and $\beta < \frac{1}{4}$ turns out to provide sufficiently strong damping for any forcing $p(t)$. To explain this informally, we note that the case of $\beta = \frac{1}{4}$ corresponds to the critically damped pendulum. More precisely, for $p \equiv 0$ the linearization $\beta\ddot{\xi} + \dot{\xi} + \xi = 0$ at $\phi = 0$ is critically damped precisely when $\beta = \frac{1}{4}$. *Condition* (i) *is thus equivalent to the requirement that the above linearization be overdamped.* Geometrically, the importance of overdamping lies in the fact that the *underdamping* causes the "rolling up" shown in Fig. 4(a), where the invariant circle is shown in the case $\beta > \frac{1}{4}$, $\gamma = 0$, $p \equiv 0$. This circle consists of the unstable manifolds of the saddle (top unstable) equilibria of the pendulum; they are rolled up due to the underdamping, causing the nonsmoothness (cf. Ref. 5), which is the first step on the route to chaos. The idea that underdamping is necessary for chaos has been expressed by Kautz and Monako.[8]

In the opposite case of small inertia versus dissipation ($\beta \ll 1$) the driven oscillator follows the forcing promptly, with inertia playing little role. Formally, we can drop the second derivative term, obtaining the Stewart-McCumber model,[16,18,19] $(1 + \gamma\cos\phi)\dot{\phi} + \sin\phi = p(t)$; the corresponding Poincaré map taking $\phi(0)$ into $\phi(2\pi/\omega)$ is now one-dimensional. Identification of ϕ modulo 2π turns it into an invertible circle map, approximating the two-dimensional map. Theorem 1 guarantees that there is no loss of information in this reduction of dimension as long as $\beta < (1 - \gamma)^2/4$. Since invertible circle maps are well understood,[17] and since the invariant circle is globally attracting, we obtain a complete picture of the full two-dimensional map.

If, however, we take $\gamma > 1$, the smallness of inertia combines with *negative* dissipation $(1 + \gamma\cos\phi < 0)$ to produce fast motions, i.e., trajectory "slices" in the phase plane, which manifest themselves in voltage spikes. Geometrically, these may result in "folds" which can destroy the one-dimensionality of the invariant circle. It should be pointed out, however, that the reduction of dimension can be carried out even if the resulting 1D map is noninvertible and possibly chaotic. In many cases there is no information loss even in such reductions of dimension (cf. Refs. 5 and 20). This reduction has been carried out rigorously and the symbolic dynamics fully analyzed for noninvertible circle maps arising in a van der Pol-type equation.

D. Extending the parameter regions of nonchaotic behavior: Large drift, etc.

One can show that for any given $p \neq 0$ the value of β can be extended beyond the value of $\frac{1}{4}$ with the smooth circle persisting. The trivial case of $p = 0$ is thus in a sense the worst for smoothness. In some particular cases one can give specific bounds on β for which the invariant circle persists. For instance, if the drift part $\bar{p} = (1/T)\int_0^T p(t)dt$ is large, then β can be large. The same is true if the oscillatory part $p_0(t) = p(t) - \bar{p}$ has large area under the positive part of its graph, with some mild extra assumptions. For the case of $p(t) = i_0 + i_1\sin\omega t$, for instance, large i_0 or i_1 allow for large β. Specific inequalities will be given elsewhere.

III. PROOFS AND MOTIVATION

A. Proof of theorem 2

As the first step, we observe that conditions (i) and (ii) imply the following third condition.

(iii) There exists a strip S in $\mathbb{R}^2$ bounded by two curves $C_+ = [(\phi, \psi): \psi = U(\phi)]$, $C_- = [(\phi, \psi): \psi = L(\phi)]$ with $U(\phi) > L(\phi)$, $U(\phi + 2\pi) = U(\phi) + 2\pi$, $L(\phi + 2\pi) = L(\phi) + 2\pi$, and with $\zeta_- < L'(\phi) < \zeta_+$, $\zeta_- < U'(\phi) < \zeta_+$ such that $PS \subset S$. The implication (i) and (ii) $\Longrightarrow$ (iii) is proven in the Appendix at the end of the paper. It is also not difficult to verify (iii) directly from Eq. (3), although doing so is redundant if (i) and (ii) have been verified.

We will show that the iterates $P^n S$ of the strip are nested and in the limit shrink to a curve which consequently must be invariant under P. To that end we observe that since the slopes of the tangents to C_+ lie between ζ_- and ζ_+ by (iii), the same must hold for all iterates $P^n C_+ (n > 0)$ by (i). In particular, every iterate $P^n C_+$ is a graph of a single-valued function $\psi = U_n(\phi)$. Similarly, $P^n C_-$ is a graph of some function $\psi = L_n(\phi)$.

As a decreasing sequence of Lipshitz functions bounded below by $L_1(\phi)$, $U_n(\phi)$ has a uniform limit $U(\phi)$. Similarly, let $L(\phi) = \lim_{n \to \infty} L_n(\phi)$; we have $L(\phi) \le U(\phi)$ for all ϕ. We show now that in fact $L(\phi) \equiv U(\phi)$; this would prove then that the invariant strip is actually an invariant circle.

If for some ϕ the inequality $U(\phi) > L(\phi)$ were to hold, the area of the annular region $0 \le \phi \le 2\pi$, $L(\phi) \le \psi \le U(\phi)$ would be positive. But an invariant set cannot have a positive area by the dissipative property (ii). This completes the proof.

B. Proof of theorem 1

To prove the existence of an invariant circle it suffices to demonstrate that the map P associated with Eq. (3) satisfies the two conditions of theorem 2. To verify the sector condition (i) we observe that the image $(\xi_1,\eta_1)=(dP_x)(\xi_0,\eta_0)$ of a tangent vector (ξ_0,η_0) under the linearization of P at $x\in\mathbb{R}^2$ is given by $(\xi_1,\eta_1)=(\xi(2\pi/\omega),\eta(2\pi/\omega))$, where $(\xi(t),\eta(t))$ is the solution of the linearized system

$$\dot{\xi}=\frac{1}{\beta}[\eta-(1+\gamma\,\cos\phi)\xi]\ ,$$
$$\dot{\eta}=-\cos\phi\,\xi$$

(5)

with $(\xi(0),\eta(0))=(\xi_0,\eta_0)$. Here $(\phi(t),\psi(t))$ solves Eq. (3) with $(\phi(0),\psi(0))=x$. To verify the sector condition (i) it suffices to show that the flow of the linearized Equation (5) crosses into the sector in Fig. 3 with boundaries $\eta/\xi=\zeta_\pm$; indeed, at the end of the period then any vector starting in the sector will remain there. Slope $\zeta(t)=\eta(t)/\xi(t)$ satisfies a Ricatti equation

$$\dot{\zeta}=-\frac{1}{\beta}\zeta^2+\frac{1}{\beta}(1+\gamma\,\cos\phi)\zeta-\cos\phi\equiv R(\zeta,t)\ ;$$

(6)

we observe that the flow of this nonautonomous equation crosses the fixed interval $[(1-\gamma)/2,2(1+\gamma)]$ inwards for any t; indeed, for $\zeta=(1-\gamma)/2$,

$$\dot{\zeta}=R\left[\frac{1-\gamma}{2},t\right]>-\frac{1}{\beta}\left[\frac{1-\gamma}{2}\right]^2+\frac{1}{\beta}(1-\gamma)\frac{1-\gamma}{2}-1$$

$$=\frac{(1-\gamma)^2}{4\beta}-1>0\ .$$

Similarly, one checks that $\dot{\zeta}<0$ for $\zeta=2(1+\gamma)$. Thus if $\zeta(0)=(\eta_0/\xi_0)\in(\zeta_-,\zeta_+)$ then $\zeta(2\pi/\omega)=\eta_1/\xi_1\in(\zeta_-,\zeta_+)$. This shows that any vector (ξ,η) starting in the sector remains there, which proves the sector condition (i).

The dissipative property (ii) follows directly from the fact that the trace of the coefficient matrix $A(t)$ in (5) is negative

$$\text{tr}\,A(t)=-\frac{1}{\beta}(1+\gamma\,\cos\phi)\leq-\frac{1}{\beta}(1-\gamma)<0\ ,$$

and thus

$$\det dP=\exp\left[\int_0^{2\pi/\omega}\text{tr}\,A(t)dt\right]\leq e^{-(1-\gamma)/\beta}<1\ .$$
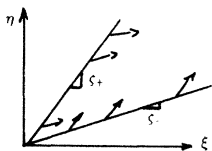
Remark 3: High inductive coupling $\gamma>1$. For $\gamma>1$ the above argument fails, since we may have positive divergence $1+\gamma\,\cos\phi>0$. This does not imply, however, that the dissipative property (ii) fails; even for $\gamma>1$ it may still persist, although the argument will have to be extended. For instance, if $p(t)$ has a large drift component, the dissipative condition (i) will hold even for $\gamma>1$. The precise estimates and arguments will be discussed elsewhere.

To demonstrate the estimate on the curve $f(\phi)$, we notice that the deviation $\Delta=\psi-\Phi(\phi)$ satisfies

$$\dot{\Delta}=-\sin\phi+p(t)-\frac{1}{\beta}(1+\gamma\,\cos\phi)\Delta\ ,$$

so that for positive deviations $\Delta>0$ we have

$$\dot{\Delta}<1+M-\frac{1}{\beta}(1-\gamma)\Delta\ ,$$

while for $\Delta<0$ the lower bound

$$\dot{\Delta}>-1+m-\frac{1}{\beta}(1-\gamma)\Delta$$

holds. These inequalities show that Δ must enter the desired interval $[\beta(m-1)/(1+\gamma),\beta(M+1)/(1-\gamma)]$.

We give now *an informal explanation of the high smoothness for large β;* the rigorous proof can be obtained by repeating the argument of Moser.[21] Assume that there exists an invariant circle as in theorem 1, and that the rotation number is rational; the circle map must have (generically, at least) a sink-saddle pair of periodic points, which are therefore fixed under some iterate $Q=P^n$ of the Poincaré map [Fig. 4(b)]. Choose the origin of the new coordinate system at the node and let the x and y axes be tangent to the weak and strong eigendirections of the linearized map dQ. We note that the sink cannot have imaginary eigenvalues, as this would cause the "roll-up" as in Fig. 4(a). Let $0<\mu<\lambda<1$ be the "vertical" and "horizontal" eigenvalues of dQ at the origin. The invariant circle in the neighborhood of the origin can be written as $y=cx^\alpha+\cdots$, with $\cdots$ denoting higher-order terms. From the invariance assumption, $\mu y=c(\lambda x)^\alpha+\cdots$, we find that $\alpha=\ln\mu/\ln\lambda>1$.

The crucial point determining the degree of smoothness is the fact that the value of the coefficient c for $x>0$ is different in general from the value for $x<0$. Thus only α derivatives at the origin on the left and on the right are expected to match. Now, $\alpha=\ln\mu/\ln\lambda$ is proportional to $1/\beta$, since the latter gives the order of

FIG. 3. Flow of the linearized equation (5) crosses into the strip, as follows from the fact that the slope ζ satisfies the Ricatti equation (6) whose one-dimensional flow crosses into the segment (ζ_-,ζ_+).

FIG. 4. (a) Roll up of the invariant curve due to underdamping. (b) Smoothness of the invariant curve is determined by $\alpha=\ln\mu/\ln\lambda$.

the exponential rate of contraction toward the invariant circle.

The above reasoning can be made precise; alternatively, a rigorous smoothness argument can be made following Moser,[21] pp. 82 and 83; the key property of the map used in both arguments is the domination of contraction within the circle by the contraction in the transversal direction.

Remark 4: Higher resonances and smoothness. If the rotation number is close to an irrational, then the above-mentioned internal contraction rate λ is close to 1, making the smoothness rate α large. The large drift component will also result in large α.

ACKNOWLEDGMENTS

APPENDIX: PROOF OF THE IMPLICATION
(i) AND (ii)⟹(iii)

Both functions $U(\phi)$ and $V(\phi)$ can actually be chosen linear, $U(\phi)=\phi+U$, $L(\phi)=\phi-L$, where U and L are constants. To prove that (i) and (ii) imply (iii), we will consider an annulus bounded by two circles $\psi=\phi\equiv f_1(\phi)$, $\psi=\phi+U\equiv f_2(\phi)$ which its image bounded by the curves $\psi=g_1(\phi)$ and $\psi=g_2(\phi)$ and show that

the top boundary moves down, i.e., $g_2(\phi)<f_2(\phi)$, provided U is chosen large enough. Heuristically, since the image boundaries still have slopes between ζ_- and ζ_+, and since the area decreases by the factor of c at least, it is reasonable to state that the height of any annulus shrinks by c plus a bounded error; this suggests (in analogy with the contraction mapping principle) that high lines $(U\gg1)$ are moved down under P, while low lines $(L\gg1)$ are moved up. To make this argument rigorous, we observe the following.

(a) For the areas A_0 and A_1 of the annulus and of its image, condition (ii) implies that $A_1<cA_0$.

(b) $A_1=\int_0^{2\pi}[g_2(\phi)-g_1(\phi)]d\phi>2\pi\min(g_2-g_1)$. Here and below, maxima and minima are taken over the interval $(0,2\pi)$.

(c) $\min(g_2-g_1)>\max(g_2-g_1)-2\pi(\zeta_+-\zeta_-)$. This follows from condition (i).

(d) $\max(g_2-g_1)>\max g_2-\min g_1$.

Applying (a), (b), (c), and (d) in that order, we obtain

$$\frac{1}{2\pi}cA_0>\frac{1}{2\pi}A_1>\min(g_2-g_1)$$

$$>\max(g_2-g_1)-2\pi(\zeta_+-\zeta_-)$$

$$>\max g_2-\min g_1-2\pi(\zeta_+-\zeta_-),$$

or, using $A_0=2\pi U$,

$$\max g_2<cU+\min g_1+2\pi(\zeta_+-\zeta_-)<U\equiv\min f_2$$

if U is large enough (g_1 is independent of U), showing that the top boundary moves down. The corresponding argument for the lower boundary $\psi=\phi-L$ is completely analogous. The proof of (iii) is complete.

Remark 5. After this work was completed, I received an unpublished report[23] by Min, Xian, and Jinyan in which a result similar to that of theorem 1 is obtained.

[1] G. Gruñer and A. Zettl, Phys. Rep. **119**, 118 (1985).

[2] M. van Veldhuizen and H. A. Fowler, Phys. Rev. B **31**, 5805 (1985).

[3] P. Bak, T. Bohr, H. Jensen, and P. V. Christiansen, Solid State Commun. **51**, 231 (1984).

[4] H. Seifert and C. Noldeke, in *Proceedings of the 17th International Conference on Low Temperature Physics, LT-17*, edited by U. Eckern, A. Schmid, W. Weber, and H. Wühl (North-Holland, Amsterdam, 1984), p. 1135.

[5] T. Bohr, P. Bak, and M. H. Jensen, Phys. Rev. A **30**, 1970 (1984).

[6] P. Bak, T. Bohr, and M. H. Jensen, Phys. Scr. T **9**, 50 (1985).

[7] M. J. Kajanto and M. M. Salomaa, Solid State Commun. **53**, 99 (1985).

[8] R. L. Kautz and R. Monako, J. Appl. Phys. **57**, 875 (1985).

[9] D.-R. He, W. J. Yeh, and Y. H. Kao, Phys. Rev. B **31**, 1359 (1985).

[10] D. G. McDonald and N. V. Frederick, Appl. Phys. Lett. **47**, 530 (1985).

[11] Ch. Noldeke and H. Seifert, Phys. Lett. **109A**, 401 (1985).

[12] A. H. MacDonald and M. Plischke, Phys. Rev. B **27**, 201 (1983).

[13] H. Tao *et al.*, Chin. Phys. Lett. **3**, 349 (1986).

[14] N. Levinson, Ann. Math. **52(3)**, 727 (1950).

[15] J. Guckenheimer and P. Holmes, *Nonlinear Oscillations, Dynamical Systems and Bifurcations of Vector Fields* (Springer, Berlin, 1983).

[16] A. A. Abidi and L. O. Chua, Electron. Circuits Syst. **3**, 186 (1979).

[17] V. I. Arnold, *Geometrical Methods in the Theory of Ordinary Differential Equations* (Springer-Verlag, Berlin, 1983).

[18] W. C. Stewart, Appl. Phys. Lett. **12**, 277 (1981).

[19] D. E. McCumber, J. Appl. Phys. **39**, 3113 (1968).

[20] M. Levi, Mem. Am. Math. Soc. **32**, 1 (1981).

[21] J. K. Moser, *Stable and Random Motions in Dynamical Systems, Study 77* (Princeton University Press, Princeton, NJ, 1973), pp. 82 and 83.

[22] M. Levi, F. C. Hoppensteadt, and W. L. Miranker, Q. Appl. Math. **167**, 176 (1978).

[23] Qian Min, Shen Wen Xian, and Zhang Jinyan, J. Diff. Eqs. (to be published).